PERIODIC MOTION AND BIFURCATIONS INDUCED BY THE PAINLEVÉ PARADOX

R. I. LEINE[a]*, **B. BROGLIATO**[b], **H. NIJMEIJER**[a]

[a] *Department of Mechanical Engineering,*
Eindhoven University of Technology,
P.O. Box 513, 5600 MB Eindhoven, The Netherlands
Email: R.I.Leine@tue.nl

[b] *INRIA Rhône-Alpes,*
ZIRST Montbonnot, 655 avenue de l'Europe,
38334, Saint Ismier Cedex, France
Email: Bernard.Brogliato@inrialpes.fr

1 SUMMARY

In this paper we study the periodic motion and bifurcations of the Frictional Impact Oscillator, which consists of an object with normal and tangential degrees of freedom that comes in contact with a rigid surface. The Frictional Impact Oscillator contains the basic mechanism for a hopping phenomenon observed in many practical applications. We will show that the hopping or bouncing motion in this type of systems is closely related to the Painlevé paradox. A dynamical system exhibiting the Painlevé paradox has nonuniqueness and nonexistence of solutions in certain sliding modes. Furthermore, we will show that this type of systems can exhibit the Painlevé paradox for physically realistic values of the friction coefficient.

2 INTRODUCTION

If a finger is pushed over a table, then a hopping motion of the finger can be observed when the finger and table are sufficiently rough. The same phenomenon occurs when a piece of chalk is pushed over the blackboard, in brake systems and robotic manipulators which touch a surface. In this paper we will study a Frictional Impact Oscillator, which consists of a rigid object with normal and tangential degrees of freedom that comes in contact with a rigid surface. The Frictional Impact Oscillator, introduced in this paper, contains the basic mechanism for the hopping phenomenon observed in many practical applications. We will show that the hopping or bouncing motion in this type of systems is closely related to the Painlevé paradox. Furthermore, we will show that this type of systems can exhibit the Painlevé paradox for arbitrary values of the friction coefficient.

The rigid multibody theory [1, 4, 5, 8, 11], which assumes instantaneous impact between rigid bodies and Amontons-Coulomb friction model in tangential direction, provides a good approach to study the dynamics when one is interested in the global motion of the system. Mechanical systems with friction and impact, modelled with a rigid multibody approach, belong to the class of hybrid systems (i.e. systems with a mixed continuous and discrete nature in time). The transitions in time from one hybrid mode to another (e.g. from contact to detachment or stick to slip) demand the choice of the next hybrid mode. A rigorous way to perform this search is to formulate the problem as a Linear Complementarity problem (LCP). The solution of the LCP can be nonunique, giving

*This research work was performed during a stay of the first author at INRIA Rhône-Alpes, France.

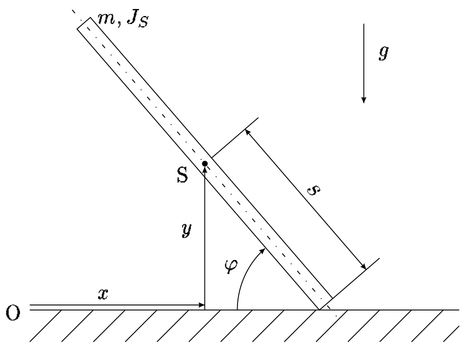

Figure 3.1: The classical Painlevé example.

an undeterminate next hybrid mode, and the solution of the LCP may even not exist, which leads to inconsistency in the model. The occurrence of inconsistency in a mechanical rigid multibody system due to friction is known as the *Painlevé paradox* [10]. A number of studies show that inconsistencies occur in the classical Painlevé example when the friction coefficient μ is larger than $\frac{4}{3}$ [3, 6, 7]. New results on how the solution of the classical Painlevé example passes singular points in the sliding mode were presented in [2].

The critical value of $\frac{4}{3}$ is very large and not likely to occur in physical situations. We will show that the Painlevé paradox can occur for arbitrary (positive) values of the friction coefficient. The notation as well as the methods of [3, 11] are used for the dynamics of rigid multibody systems with impact and friction.

3 THE CLASSICAL PAINLEVÉ EXAMPLE

Consider a rigid homogeneous slender rod with mass m, length $2s$ and inertia $J_S = \frac{1}{3}ms^2$ (Figure 3.1). The rod is sliding with one tip over a rigid ground with friction coefficient μ. The system has three degrees of freedom, $\boldsymbol{q} = \begin{bmatrix} x & y & \varphi \end{bmatrix}^{\mathrm{T}}$. The normal contact distance and tangential contact velocity are $g_N = y - s\sin\varphi$ and $\dot{g}_T = \dot{x} - s\dot{\varphi}\sin\varphi$.

It is relatively easy to show that a dynamic frictional catastrophe can occur in this simple system. Assume that the rod is sliding from over the ground in forward direction, i.e. $g_N = 0$, $\dot{g}_N = 0$ and $\dot{g}_T > 0$. It therefore holds that $\lambda_T = -\mu\lambda_N$. The equations of motion become in the forward sliding mode

$$\begin{aligned} m\ddot{x} &= -\mu\lambda_N \\ m\ddot{y} &= -mg + \lambda_N \\ J_S\ddot{\varphi} &= s(-\cos\varphi + \mu\sin\varphi)\lambda_N . \end{aligned} \tag{3.1}$$

The rod remains in sliding contact when $\ddot{g}_N = 0$ and will detach when $\ddot{g}_N > 0$, with

$$\ddot{g}_N = \ddot{y} - s\cos\varphi\ddot{\varphi} + s\dot{\varphi}^2\sin\varphi. \tag{3.2}$$

The normal contact acceleration becomes in the forward sliding mode (substituting (3.1) in (3.2))

$$\ddot{g}_N = A\lambda_N + b, \tag{3.3}$$

with $A(\varphi) = \frac{1}{m}\big(1+3\cos\varphi(\cos\varphi-\mu\sin\varphi)\big)$ and $b(\varphi,\dot{\varphi}) = s\dot{\varphi}^2\sin\varphi - g$. Between the normal contact acceleration $\ddot{g}_N$ and the normal contact force λ_N the following complementarity conditions hold

$$0 \leq \ddot{g}_N \perp \lambda_N \geq 0. \tag{3.4}$$

The complementarity conditions (3.4) express that if the contact detaches, $\ddot{g}_N > 0$, then it must hold that $\lambda_N = 0$, while if the normal contact force is positive $\lambda_N > 0$ the contact remains closed $\ddot{g}_N = 0$. The linear equation (3.3) together with the complementarity conditions (3.4) gives a scalar Linear Complementarity Problem (LCP) for the detachment of the rod in the forward sliding mode. The scalar LCP with $\ddot{g}_N = A\lambda_N + b$, $0 \leq \ddot{g}_N \perp \lambda_N \geq 0$ has a unique solution for $A > 0$, two solutions for $A < 0 \wedge b > 0$, no solution for $A < 0 \wedge b < 0$ or infinitely many solutions for $A = b = 0$ (hyperstatic case). The occurrence of inconsistency (the LCP has no solution) and indeterminacy (nonuniqueness of solutions) is called the Painlevé paradox [2].

The Painlevé paradox will occur when $A(\varphi)$ becomes negative, which happens for large enough values of μ. The critical value of μ for which $A(\varphi) = 0$ occurs at $\mu = \mu_c(\varphi)$ with

$$\mu_c(\varphi) = \frac{1 + 3\cos^2\varphi}{3\sin\varphi\cos\varphi}. \tag{3.5}$$

The critical friction $\mu_c(\varphi)$ coefficient is minimal for $\varphi = \arctan 2$, giving $\mu_{c\min} = \frac{4}{3}$. This minimal critical friction coefficient changes for other ratios of $\frac{ms^2}{J_S}$ but will always be larger than 1.

4 THE FRICTIONAL IMPACT OSCILLATOR

A human finger, pushed over a table, may exhibit periodic motion with stick and slip phases. When the friction between the finger-tip and the table is sufficiently high, even periodic motion may be observed with phases where the finger is not in contact with the table, i.e. the finger detaches from the table causing a 'flight' phase after which an impact occurs to another phase of the periodic motion. We will study a simple system, called the Frictional Impact Oscillator, which exhibits the same phenomenon and show how it is related to the Painlevé paradox.

4.1 Model

The Frictional Impact Oscillator is depicted in Figure 4.1. The system consists of a mass-spring-damper system (with coordinate y and constants m_2, k, c), which can be looked upon as the 'hand'. A massless rigid bar, representing the 'finger' is attached by a hinge to the 'hand'. The hinge can only move in the vertical direction by a displacement y. The bar is mounted at the hinge by a rotational spring and dashpot (k_φ, c_φ). A mass m_1 is located at the tip of the bar. The springs k and k_φ are unstressed when $y = 0$ and $\varphi = \varphi_0$ respectively. The tip of the bar can make contact with a belt, moving at constant velocity v_{dr}. The contact is regarded to be completely inelastic. Pure Amontons-Coulomb friction is assumed without Stribeck effect (μ is not dependent on the relative velocity). The normal contact distance and tangential contact velocity are

$$g_N = l(1 - \cos\varphi) + y, \quad \dot{g}_T = l\dot{\varphi}\cos\varphi + v_{\mathrm{dr}}. \tag{4.1}$$

Lagrange's equations of motion can be put in the form $\boldsymbol{M}(\boldsymbol{q})\ddot{\boldsymbol{q}} - \boldsymbol{h}(\boldsymbol{q}, \dot{\boldsymbol{q}}) - \boldsymbol{W}_N(\boldsymbol{q})\lambda_N - \boldsymbol{W}_T(\boldsymbol{q})\lambda_T = \boldsymbol{0}$, with $\boldsymbol{q} = \begin{bmatrix}\varphi & y\end{bmatrix}^{\mathrm{T}}$, where λ_N and λ_T are the normal and tangential contact forces. We can express the contact velocities and accelerations in the generalized accelerations by

$$\begin{bmatrix}\dot{g}_N \\ \dot{g}_T\end{bmatrix} = \begin{bmatrix}\boldsymbol{W}_N^{\mathrm{T}} \\ \boldsymbol{W}_T^{\mathrm{T}}\end{bmatrix}\dot{\boldsymbol{q}} + \begin{bmatrix}\tilde{w}_N \\ \tilde{w}_T\end{bmatrix}, \qquad \begin{bmatrix}\ddot{g}_N \\ \ddot{g}_T\end{bmatrix} = \begin{bmatrix}\boldsymbol{W}_N^{\mathrm{T}} \\ \boldsymbol{W}_T^{\mathrm{T}}\end{bmatrix}\ddot{\boldsymbol{q}} + \begin{bmatrix}\bar{w}_N \\ \bar{w}_T\end{bmatrix}. \tag{4.2}$$

The system matrices and vectors of the Frictional Impact Oscillator become

$$\boldsymbol{M} = \begin{bmatrix} m_1 l^2 & m_1 l \sin\varphi \\ m_1 l\sin\varphi & m_1 + m_2\end{bmatrix}, \qquad \boldsymbol{h} = \begin{bmatrix} -k_\varphi(\varphi - \varphi_0) - c_\varphi\dot{\varphi} - m_1 g l \sin\varphi \\ -ky - c\dot{y} - (m_1 + m_2)g - m_1 l\cos\varphi\,\dot{\varphi}^2\end{bmatrix}, \tag{4.3}$$

$$\boldsymbol{W}_N = \begin{bmatrix} l\sin\varphi \\ 1\end{bmatrix}, \boldsymbol{W}_T = \begin{bmatrix} l\cos\varphi \\ 0\end{bmatrix}, \tilde{w}_N = 0, \bar{w}_N = l\dot{\varphi}^2\cos\varphi, \tilde{w}_T = v_{\mathrm{dr}}, \bar{w}_T = -l\dot{\varphi}^2\sin\varphi. \tag{4.4}$$

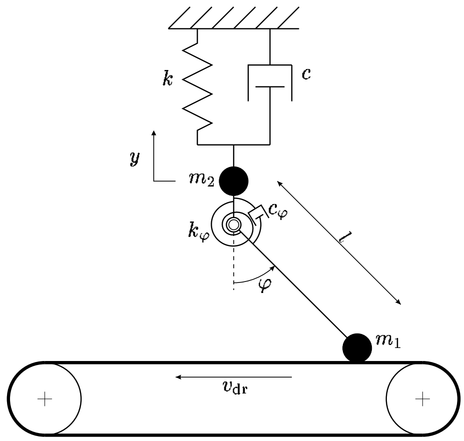

Figure 4.1: The Frictional Impact Oscillator.

4.2 Forward Slip, $\dot{g}_T > 0$

The motion of the system in the forward slip mode is constraint with $\lambda_N \geq 0$ and $\lambda_T = -\mu\lambda_N$. The equations of motion in the forward slip mode become

$$\begin{aligned} m_1 l^2 \ddot{\varphi} + m_1 l \sin\varphi\, \ddot{y} + c_\varphi \dot{\varphi} + k_\varphi(\varphi - \varphi_0) &= l(\sin\varphi - \mu\cos\varphi)\lambda_N - m_1 g l \sin\varphi \\ m_1 l \sin\varphi\, \ddot{\varphi} + (m_1 + m_2)\ddot{y} + c\dot{y} + ky + m_1 l \cos\varphi\, \dot{\varphi}^2 &= \lambda_N - (m_1 + m_2)g. \end{aligned} \tag{4.5}$$

Elimination of λ_N together with the conditions $g_N = \dot{g}_N = \ddot{g}_N = 0$ gives a second order differential equation

$$\mathcal{M}(\varphi)\ddot{\varphi} + \mathcal{D}(\varphi)\dot{\varphi}^2 + \mathcal{C}(\varphi)\dot{\varphi} + \mathcal{F}(\varphi) = 0, \tag{4.6}$$

with

$$\begin{aligned} \mathcal{M}(\varphi) &= \big(m_1 \cos^2\varphi + m_2 \sin\varphi(\sin\varphi - \mu\cos\varphi)\big)l^2 \\ \mathcal{D}(\varphi) &= \big((-m_1 + m_2)\sin\varphi\cos\varphi - m_2\mu\cos^2\varphi\big)l^2 \\ \mathcal{C}(\varphi) &= c_\varphi + cl^2 \sin\varphi(\sin\varphi - \mu\cos\varphi) \\ \mathcal{F}(\varphi) &= k_\varphi(\varphi - \varphi_0) + kl^2(1 - \cos\varphi)(\sin\varphi - \mu\cos\varphi) + \big((m_1 + m_2)\mu\cos\varphi - m_2\sin\varphi\big)lg. \end{aligned} \tag{4.7}$$

The system can have (multiple) equilibria φ_{eq} in the forward sliding mode, which obey $\mathcal{F}(\varphi_{eq}) = 0$ and a nonzero contact force $\lambda_N = -kl(1 - \cos\varphi_{eq}) + (m_1 + m_2)g \geq 0$. If the condition $\mathcal{K}(\varphi) = \frac{\partial\mathcal{F}(\varphi)}{\partial\varphi} > 0, \quad \forall\varphi$ holds then at most one equilibrium in the forward sliding mode exists. We assume in the forthcoming that k_φ is chosen large enough that indeed $\mathcal{K}(\varphi) > 0$ for all φ of interest. This means that the unique equilibrium φ_{eq}, if it exists and obeys $\lambda_N > 0$, must be close to φ_0. The eigenvalue problem of the linearization around the equilibrium yields

$$\mathcal{M}(\varphi_{eq})\lambda^2 + \mathcal{C}(\varphi_{eq})\lambda + \mathcal{K}(\varphi_{eq}) = 0. \tag{4.8}$$

The equilibrium is stable if $\mathcal{M}(\varphi_{eq}) > 0$, $\mathcal{C}(\varphi_{eq}) > 0$ and $\mathcal{K}(\varphi_{eq}) > 0$ or $\mathcal{M}(\varphi_{eq}) < 0$, $\mathcal{C}(\varphi_{eq}) < 0$ and $\mathcal{K}(\varphi_{eq}) < 0$. Note that the friction coefficient μ can cause a positive feedback of the damping forces. The equilibrium undergoes a Hopf bifurcation for $\mathcal{M}(\varphi_{eq}) > 0$, $\mathcal{K}(\varphi_{eq}) > 0$ when the friction coefficient μ passes the critical value

$$\mu_d = \tan\varphi_{eq} + \frac{c_\varphi}{cl^2 \sin\varphi_{eq}\cos\varphi_{eq}}, \tag{4.9}$$

for which $\mathcal{C}(\varphi_{eq}) = 0$.[1] The value of $\mathcal{M}(\varphi_{eq})$ becomes zero when $\mu = \tan\varphi_{eq} + \frac{m_1}{m_2}\frac{1}{\tan\varphi_{eq}}$, which is in fact the Painlevé paradox.

[1] If μ *passes* μ_d, then it follows that $\mathcal{C}(\varphi_{eq})$ changes sign. A pair of complex conjugated eigenvalues move therefore *through* the imaginary axis, implying a Hopf bifurcation.

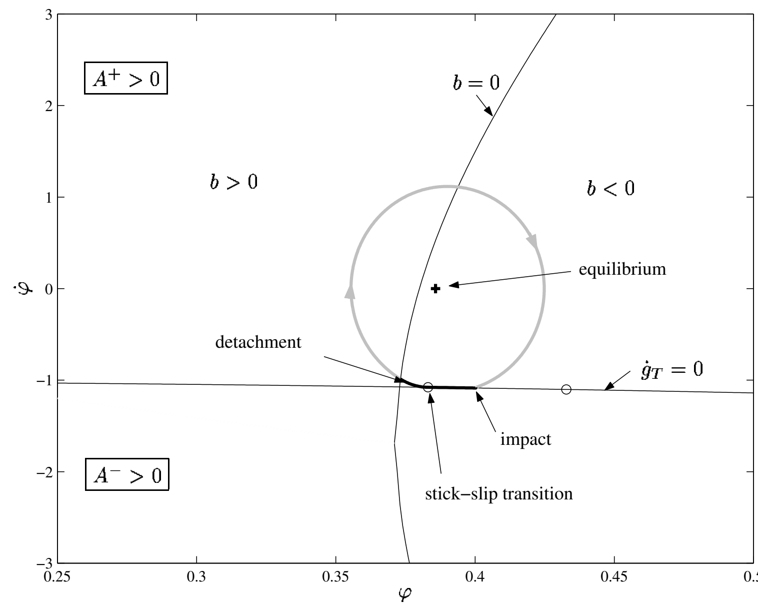

Figure 4.2: The $(\varphi, \dot{\varphi})$-plane of the Frictional Impact Oscillator, $\mu = 0.5$.

4.3 Painlevé paradox

In this subsection we will study the Painlevé paradox in the forward and backward sliding mode with similar techniques as presented in [2].

The solution remains in the forward sliding mode if $\dot{g}_T > 0$ and $\ddot{g}_N = 0$ and in the backward sliding mode if $\dot{g}_T < 0$ and $\ddot{g}_N = 0$. The body detaches from the belt when $\ddot{g}_N > 0$. For the normal contact acceleration $\ddot{g}_N$ holds $\ddot{g}_N = l \sin\varphi\, \ddot{\varphi} + \ddot{y} + l\cos\varphi\, \dot{\varphi}^2$. Substituting the equation of motion in (4.2) together with $g_N = \dot{g}_N = 0$ gives

$$\ddot{g}_N = \begin{cases} A^+\lambda_N + b, & \dot{g}_T > 0 \\ A^-\lambda_N + b, & \dot{g}_T < 0 \end{cases}, \tag{4.10}$$

with

$$A^\pm(\varphi) = \boldsymbol{W}_N^{\mathrm{T}} \boldsymbol{M}^{-1}(\boldsymbol{W}_N \mp \mu \boldsymbol{W}_T) = \frac{\cos^2\varphi}{N(\varphi)}\Big(1 + \frac{m_2}{m_1}\tan\varphi(\tan\varphi \mp \mu)\Big), \tag{4.11}$$

$$\begin{aligned} b(\varphi, \dot{\varphi}) &= \boldsymbol{W}_N^{\mathrm{T}} \boldsymbol{M}^{-1}\boldsymbol{h} + \bar{\boldsymbol{w}}_N \\ &= \frac{\cos^2\varphi}{N(\varphi)}\Big(-\frac{m_2}{m_1}\frac{\tan\varphi}{l\cos\varphi}\big(c_\varphi\dot{\varphi} + k_\varphi(\varphi - \varphi_0)\big) + cl\sin\varphi\,\dot{\varphi} + kl(1 - \cos\varphi) + \frac{m_2 l}{\cos\varphi}\dot{\varphi}^2\Big) - g \end{aligned} \tag{4.12}$$

and $N(\varphi) = m_1\cos^2\varphi + m_2$. The notation A^+ is used to denote the value of A in the forward sliding mode, while A^- will be used for the backward sliding mode. Note that $A^\pm$ are functions of φ and μ, and b is a function of φ and $\dot{\varphi}$. The linear equation (4.10) gives together with the complementarity conditions $0 \le \ddot{g}_N \perp \lambda_N \ge 0$ a scalar Linear Complementarity Problem for the detachment in the forward and backward sliding mode.

The Painlevé paradox occurs in the forward sliding mode when $A^+(\varphi)$ becomes negative, leading to inconsistency or indeterminacy of the forward sliding mode (depending on the sign of $b(\varphi, \dot{\varphi})$). The value $A^+(\varphi)$ can become negative for sufficiently large values of the friction coefficient μ. The critical value occurs at $\mu = \mu_c^+(\varphi)$ for which $A^+(\varphi) = 0$,

$$\mu_c^+(\varphi) = \tan\varphi + \frac{m_1}{m_2}\frac{1}{\tan\varphi}. \tag{4.13}$$

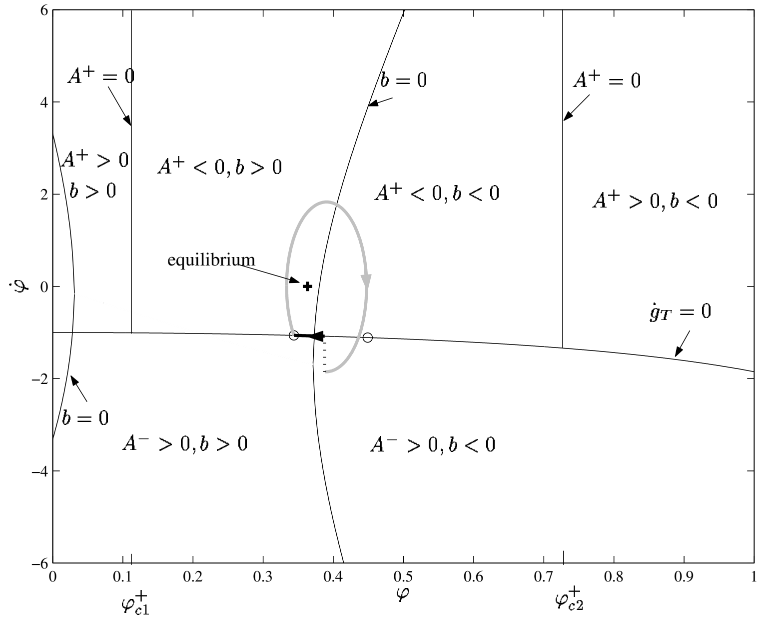

Figure 4.3: The $(\varphi, \dot{\varphi})$-plane of the Frictional Impact Oscillator, $\mu = 1$.

The critical value $\mu_c^+(\varphi)$ is minimal when $\varphi = \arctan\sqrt{\frac{m_1}{m_2}}$ giving

$$\mu_{\text{cmin}} = 2\sqrt{\frac{m_1}{m_2}}. \tag{4.14}$$

For $\mu \geq \mu_{\text{cmin}}$ there exists an interval of $\varphi^+_{c1} < \varphi < \varphi^+_{c2}$ for which $A^+ < 0$ with

$$\varphi^+_{c1} = \arctan\left(\frac{1}{2}\mu + \sqrt{\frac{1}{4}\mu^2 - \frac{m_1}{m_2}}\right), \qquad \varphi^+_{c2} = \arctan\left(\frac{1}{2}\mu - \sqrt{\frac{1}{4}\mu^2 - \frac{m_1}{m_2}}\right). \tag{4.15}$$

With respect to the previous section we have to remark the following

1. It holds that $A^+(\varphi) = 0$ if and only if $\mathcal{M}(\varphi) = 0$.

2. Let $\mu = \mu_c^+ > 0$ and be bounded such that $A^+(\varphi) = 0$. Then it holds that $b(\varphi, \dot{\varphi}) = 0$ if and only if $\mathcal{D}(\varphi)\dot{\varphi}^2 + \mathcal{C}(\varphi)\dot{\varphi} + \mathcal{F}(\varphi) = 0$.

We can conclude that when φ is such that $A^+ = 0$, then the slip equation (4.6) is fulfilled only when $b = 0$.

4.4 Analysis of Periodic Motion

The Frictional Impact Oscillator can exhibit periodic motion with slip, stick and flight phases. We will explore how the topology of the periodic solution depends on the regions defined by the lines $A = 0$ and $b = 0$. We will consider two cases: case 1 with $\mu = 0.5 < \mu_{\text{cmin}}$ and case 2 with $\mu = 1 > \mu_{\text{cmin}}$, where $\mu_{\text{cmin}} = 0.6325$. The other parameters are $m_1 = 0.1$ kg, $m_2 = 1$ kg, $l = 1$ m, $k = 100$ N/m, $k_\varphi = 100$ Nm, $c = 10$ N/(ms), $c_\varphi = 0$ Nm/s, $\varphi_0 = \frac{\pi}{8}$, $v_{\text{dr}} = 1$ m/s, $g = 10$ Nm/s^2.

Case 1: $\mu = 0.5$. Solutions in the forward slip mode exist and are unique because $A > 0\ \forall\varphi$ for $\mu < \mu_{\text{cmin}}$. The lines $b = 0$ (4.12) and $\dot{g}_T = 0$ are drawn in the plane $(\varphi, \dot{\varphi})$ of Figure 4.2. The borders of the stick mode on the line $\dot{g}_T$ in Figure 4.2 are obtained numerically and depicted by a small circle ($\circ$). The part of the line $\dot{g}_T$ between the two $\circ$ signs is therefore the stick mode. Note that the stick mode lies, for this parameter set, totally outside the detachment region

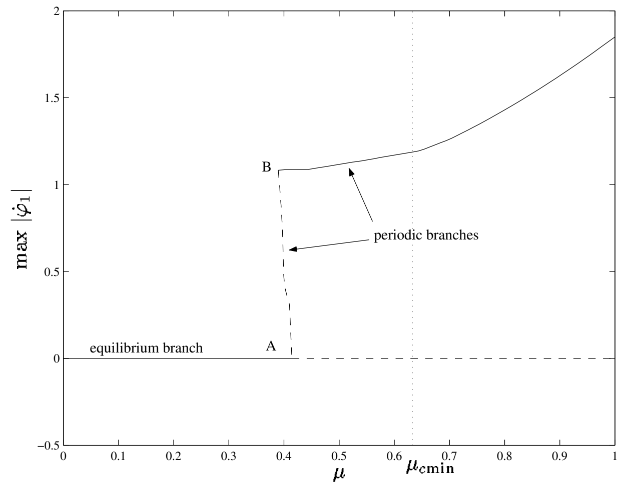

Figure 5.1: Bifurcation diagram of the Frictional Impact Oscillator.

$A^+ > 0, b > 0$. A stable periodic solution is found numerically and consists of the following phases: stick–slip–flight. The dynamics of the flight phase is not only dependent on $(\varphi, \dot{\varphi})$ and is therefore depicted in grey. The stick to slip transition occurs at the border of the stick mode. The body remains some time in forward slipping contact with the belt in the space $A^+ > 0, b < 0$ until the line $b = 0$ is hit. The sign of b changes at the line $b = 0$, giving the LCP solution $\lambda_N = 0, \ddot{g}_N > 0$, which means that the body detaches from the belt. The body remains in flight (unconstrained free motion) until an impact occurs ($g_N = 0$). The impact causes the velocities $\dot{\varphi}$ and $\dot{y}$ to jump. However, the jump is so small that the discontinuity cannot be seen at the scale of Figures 4.2. The impact results in sticking of the body to the belt.

Case 2: $\mu = 1$. Nonexistence and nonuniqueness exist for this parameter set and are depicted in Figure 4.3. The stick mode is now bordered partly by the region $A^+ < 0, b > 0$ (the indeterminate mode of the detachment LCP of the forward slip mode) and is partly bordered by the region $A^+ < 0, b < 0$ (the inconsistent mode of the detachment LCP of the forward slip mode). A periodic solution was found which contains a stick phase and a flight phase (depicted in grey). The velocity jump due to the impact is depicted by a dotted line. The impact causes the post-impact state to be in the stick mode.

5 BIFURCATIONS

The bifurcation diagram of the Frictional Impact Oscillator is depicted in Figure 5.1 taking the friction coefficient μ as bifurcation parameter. The stable periodic solution for $\mu = 0.5$ corresponds with Figure 4.2 and for $\mu = 1$ with Figure 4.3. The two periodic solutions (cases 1 and 2) are topologically different. A change in the topology of the periodic solution (from case 1 to case 2) occurs close to $\mu = \mu_{\mathrm{cmin}}$. Such a qualitative change is sometimes called bifurcation. A bifurcation in the sense that the number of coexisting equilibria or periodic solutions changes does however not occur at this point. The Painlevé paradox can however lead to a bifurcation in this sense if the parameter set is slightly different such that $\mu_d > \mu_{\mathrm{cmin}}$.

6 CONCLUSIONS

In the previous sections we analyzed the Frictional Impact Oscillator and showed that the critical friction coefficient depends only on a mass ratio and can therefore be made arbitrary small, i.e.

$\mu_{c\min} = 2\sqrt{m_1/m_2}$. The Painlevé Paradox can therefore occur at physically realistic values of the friction coefficient, which was not apparent from the classical Painlevé example.

The Frictional Impact Oscillator can be seen as a sort of archetype of systems with a frictional hopping/bouncing motion, carrying the basic mechanism for this phenomenon. We can draw a number of conclusions from the analysis of the Frictional Impact Oscillator. If the mass of the end-effector of the structure, m_1, is small with respect to the mass of the supporting structure m_2, then the Painlevé paradox can occur at physically realistic values of the friction coefficient. Hopping motion can occur when the friction coefficient μ is large enough such that either the linear damping terms vanish/become negative or the Painlevé paradox occurs. For many practical applications it might very well be that $\mu_{c\min} < \mu_d$ and that the Painlevé paradox is the actual cause of (undesirable) periodic motion. To avoid the hopping phenomenon in these type of systems, one should therefore increase the mass m_1 of the end-effector. The support stiffness k and damping c can be looked upon as the PD-action of a position controller for the link with mass m_2. When the friction is high enough such that $\mu > \tan\varphi$, then the D-action will diminish the dissipation in the system. In fact, the friction causes positive feedback, which can lead to instability of the forward sliding equilibrium.

A bifurcation diagram of the model was analyzed in Section 5. The Painlevé paradox will introduce locally nonexistence or nonuniqueness. The phase portrait of a system with the Painlevé paradox is therefore topologically different from the phase portrait of a system without the Painlevé paradox. If the Painlevé paradox occurs at a critical value of the bifurcation parameter, then a topological transition will occur at this critical point, which might lead to a bifurcation of branches of periodic solutions or equilibria, but not necessarily.

References

[1] B. Brogliato. *Nonsmooth Mechanics.* Springer, London, 2 edition, 1999.

[2] F. Génot and B. Brogliato. New results on Painlevé Paradoxes. *Eur. J. Mech.A/Solids*, 18:653–677, 1999.

[3] Ch. Glocker. *Dynamik von Starrkörpersystemen mit Reibung und Stößen*, volume 18 of *Fortschr.-Ber. VDI.* VDI Verlag, Düsseldorf, 1995.

[4] Ch. Glocker. *Set-Valued Force Laws, Dynamics of Non-Smooth Systems*, volume 1 of *Lecture Notes in Applied Mechanics.* Springer-Verlag, Berlin, 2001.

[5] R. I. Leine, Ch. Glocker, and D. H. Van Campen. Nonlinear dynamics and modeling of some wooden toys with impact and friction. *Journal of Vibration and Control*, 2002. 42 pages, accepted.

[6] P. Lötstedt. Coulomb friction in two-dimensional rigid-body systems. *Z. Angew. Math. Mech.*, 61:605–615, 1981.

[7] M. T. Mason and Y. Wang. On the inconsistency of rigid-body frictional planar machanics. *Proc. IEEE Int. Conf. Robotics and Automation*, pages 524–528, 1988.

[8] J. J. Moreau. *Unilateral contact and dry friction in finite freedom dynamics*, pages 1–82. In Moreau and Panagiotopoulos [9], 1988.

[9] J. J. Moreau and P. D. Panagiotopoulos, editors. *Non-Smooth Mechanics and Applications.* Springer, 1988.

[10] P. Painlevé. Sur les lois du frottement de glissement. *Comptes Rendu des Séances de l'Academie des Sciences*, 141:401–405 and 546–552, August 1905.

[11] F. Pfeiffer and Ch. Glocker. *Multibody dynamics with unilateral contacts.* Wiley, New York, 1996.